INTERNATIONAL BACCALAUREATE DIPLOMA PROGRAM

PHYSICS EXTENDED ESSAY

TOPIC: “Wall” Effect of Relative Radius on Relative Drag Experienced by a Sphere in a Bounded Medium.

RESEARCH QUESTION: How does the relative radius of a sphere affect the relative drag force it experiences in a bounded medium?

WORD COUNT: 3983 Words

How does the relative radius of a sphere affect the relative drag force it experiences in a bounded medium?

TABLE OF CONTENT

1. INTRODUCTION....3

2. BACKGROUND INFORMATION....4

2.1. Forces on Falling Spheres....4

2.2. Relevant Concepts in Fluid Mechanics:....5

2.2.1. Fluids and Forces....5

2.2.2. Types of Flow....6

2.3. Drag....7

2.4. Navier-Stokes Equations....9

2.5. Modelling the Wall Effect....10

2.5.1. Model....10

2.5.2. Assumptions....14

3. VARIABLES....15

3.1. Independent Variable....15

3.2. Dependent Variable....15

3.3. Controlled Variables....16

4. EXPERIMENTAL DESIGN....18

4.1. Apparatus....18

4.2. Setup....19

4.3. Video Analysis – Parameters & Calibration....21

4.4. Safety Considerations....22

5. DATA & ANALYSIS....23

5.1. Calculating Terminal Velocities....23

5.2. Calculating Viscosity....24

5.3. Calculating the Viscosity Ratio....25

5.4. Processed Data....27

5.5. Comparison with Theoretical Model....28

6. CONCLUSION....29

7. EVALUATION....30

8. FURTHER STUDIES....33

9. BIBLIOGRAPHY....34

10. APPENDIX....36

10.1. Researcher's Reflection Space....36

10.2. Derivation of Equation (21)....................39
10.3. Integration of Equation (31)....................40
10.4. Vernier Calliper Measurements....................41
10.5. Temperature Dependence of Density – Interpolation....................41
10.6. Temperature Dependence of Viscosity – Interpolation....................42
10.7. Uncertainty in c....................43
10.8. Uncertainties in Theoretical Values....................44

1. INTRODUCTION

The field of aerodynamics has fascinated humans for centuries – from flight to free fall with a parachute – and integral to it is the concept of drag.

A typical understanding of drag experienced in a fluid is that it is proportional to the velocity, as stated in Stokes' law[1]. However, various intriguing factors that non-linearly impact the accuracy and applicability of this formula exist, and these can be significant considerations in applications involving bioengineering of devices that travel in bodily vessels, or the study of the motion of sperm cells or others.

Stokes' law is applicable only in cases of laminar flow, and under these conditions, one such effect is known as *the wall effect* ("effect of finite boundaries on the drag experienced by a rigid sphere settling along the axis of cylindrical tubes")[2]. The difference between bounded and unbounded media is:

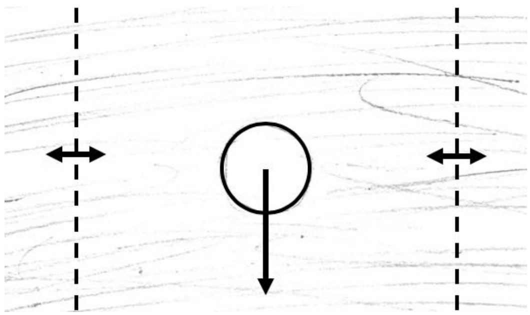

Figure 1a – Object in Unbounded Medium

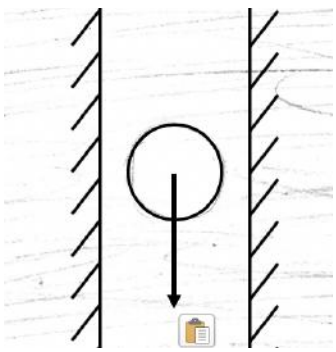

Figure 1b – Object in Bounded Medium

[1] Fowler, Michael. "Dropping the Ball (Slowly)." Stokes' Law, University of Virginia, galileo.phys.virginia.edu/classes/152.mf1i.spring02/Stokes_Law.htm.
[2] Song, Daoyun, Rakesh K. Gupta, and Rajendra P. Chhabra. "Wall effect on a spherical particle settling along the axis of cylindrical tubes filled with Carreau model fluids." Proceedings of Comsol Conference, Boston. 2011.

This essay aims to study the variation of the effect of the wall on the drag force experienced, with respect to the ratio of the object radius to the tube radius (relative radius). The dependent variable is the ratio of the drag in bounded to unbounded media, both theoretically and experimentally (relative drag).

RESEARCH QUESTION: *How does the relative radius of a sphere affect the relative drag force it experiences in a bounded medium?*

2. BACKGROUND INFORMATION

2.1. Forces on Falling Spheres

When spheres fall vertically straight through cylinders, no lateral or rotational forces act. The downward force is $F_{weight} = -mg$. Upward forces acting are drag and buoyancy ("net upward force exerted by a fluid on an object"[3]). In translational equilibrium, the object, here a sphere, travels at constant terminal velocity v_t.

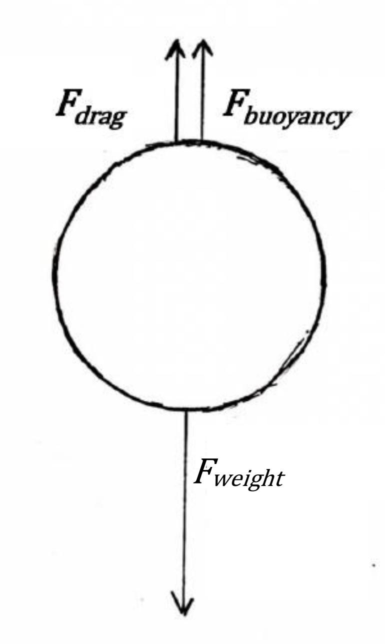

Figure 2 – Free-body diagram for falling sphere

$$F_{weight} = F_{buoyancy} + F_{drag} \tag{1}$$

$$F_{drag} = F_{weight} - F_{buoyancy} \tag{2}$$

[3] Bonk, Ryan. "Buoyancy." *The Physics of Viking Ships*, University of Alaska, Fairbanks, ffden-2.phys.uaf.edu/webproj/212_spring_2017/Ryan_Bonk/purtyWebProj/vikingSlide1.html.

The force of buoyancy is the pressure difference between the top and bottom of the sphere multiplied by the cross-sectional area this acts on[4].

$$F_{drag} = m_{sphere}g - P_{fluid} \times Area \tag{3}$$

The pressure difference in a fluid is $h\rho g$, where h is the difference in height, and ρ is the density of the fluid. Since $\rho = \frac{m}{V}$, $m = \rho V$.

$$F_{drag} = \rho_{sphere}Vg - \rho_{fluid} \times Area \times h \times g \tag{4}$$

The product of area and height is equal to the volume of fluid displaced (also *V*).

$$F_{drag} = \rho_{sphere}Vg - \rho_{fluid}Vg \tag{5}$$

For a sphere of radius r_0, $V = \frac{4}{3}\pi {r_0}^3$. Thus, in the case of a falling sphere:

$$F_{drag} = \frac{4}{3}\pi {r_0}^3 g(\rho_{sphere} - \rho_{fluid}) \tag{6}$$

2.2. Relevant Concepts in Fluid Mechanics:

2.2.1. Fluids and Forces

Fluids can refer to gases or liquids. Shear deformation in fluids arises from *shear stress* (τ/Pa), which is the force per unit are acting parallel to an infinitesimal surface element[5]. This follows the below proportionality[6]:

$$\tau \propto \frac{du}{dx} \tag{7}$$

Where *u* refers to the velocity of flow and *x* is the diameter of flow. $\frac{du}{dx}/s^{-1}$ is equal to the velocity gradient, which represents the rate of deformation in the fluid.

---

[4] Bonk, Ryan. "Buoyancy." *The Physics of Viking Ships*, University of Alaska, Fairbanks, ffden-2.phys.uaf.edu/webproj/212_spring_2017/Ryan_Bonk/purtyWebProj/vikingSlide1.html.
[5] Cimbala, John M. "What Is Fluid Mechanics?" Fluid Mechanics Electronic Learning Supplement, Pennsylvania State University, www.me.psu.edu/cimbala/Learning/Fluid/Introductory/what_is_fluid_mechanics.htm.
[6] Brennen, C.E. Internet Book on Fluid Mechanics. Dankat Publishing, 2016.

The constant of proportionality is the *dynamic viscosity* (η/Pas) (a fluid's resistance to deformation under shear stress)[7].

$$\tau = \eta \frac{du}{dx} \tag{8}$$

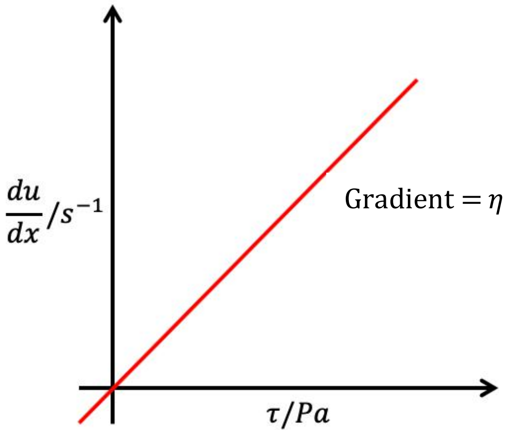

Figure 3 – Proportionality of τ *and* $\frac{du}{dx}$

In containers, *cohesive forces* act between particles of the fluid[8] and *adhesive forces* act those between two media (i.e. fluid and container)[9]. At wall interfaces, adhesive forces are dominant[10]. This causes the *no-slip* condition – fluid immediately adjacent to the wall has zero speed[11].

2.2.2. Types of Flow

- *Laminar flow*[12] occurs when a fluid flows smoothly, when viscous forces dominate inertial forces.
- *Turbulent flow*[13] is characterized by irregular fluctuations in the flow and occurs when the opposite is the case.

[7] Brennen, C.E. Internet Book on Fluid Mechanics. Dankat Publishing, 2016.
[8] Nave, R. Surface Tension, HyperPhysics, hyperphysics.phy-astr.gsu.edu/hbase/surten.html.
[9] Nave, R. Surface Tension, HyperPhysics, hyperphysics.phy-astr.gsu.edu/hbase/surten.html.
[10] Nave, R. Surface Tension, HyperPhysics, hyperphysics.phy-astr.gsu.edu/hbase/surten.html.
[11] Brennen, C.E. Internet Book on Fluid Mechanics. Dankat Publishing, 2016.
[12] Nakayama, Y. Introduction to Fluid Mechanics. Butterworth-Heinemann, an Imprint of Elsevier, 1999.
[13] Nakayama, Y. Introduction to Fluid Mechanics. Butterworth-Heinemann, an Imprint of Elsevier, 1999.

Two forces act in flowing fluids:

- *Inertial forces* result from resistance to change in momentum.[14]
- *Viscous forces* result from resistance to *flow* (shear deformation of fluid).[15]

Reynolds' Number[16] is the ratio between inertial and viscous forces, and characterizes the flow, ρ is the fluid density and d is the diameter of flow.

$$Re = \frac{\rho_l u^2}{\eta\left(\frac{u}{d}\right)} = \frac{\rho u d}{\eta} \tag{9}$$

When $Re < 1$, this indicates dominance of viscous forces and hence laminar flow – this condition is known as Stokes' flow[17]. $Re > 1$ does not necessitate turbulent flow. For flow around spheres, streamline separation around spheres, causing turbulent flow, research has shown that this does not occur until Re =17.[18]

2.3. Drag

Drag comprises of two forces:

- *Friction Drag* (arises from friction between the object and the fluid layers, and results in shear (parallel deformation), acting parallel to an infinitesimal surface element ***dA***[19] ($\tau \times Area$).
- *Pressure Drag* arises from pressure differences between the front and back of the object, and acts perpendicular to an infinitesimal surface element ***dA***[20] ($p \times Area$).

---

[14] d'Alembert, Jean-Baptiste le Rond. "Force of inertia." The Encyclopedia of Diderot & d'Alembert Collaborative Translation Project. Translated by John S.D. Glaus. Ann Arbor: Michigan Publishing, University of Michigan Library, 2006. Web. [fill in today's date in the form 18 Apr. 2009 and remove square brackets]. <http://hdl.handle.net/2027/spo.did2222.0000.714>. Trans. of "Force d'inertie," Encyclopédie ou Dictionnaire raisonné des sciences, des arts et des métiers, vol. 7. Paris, 1757.

[15] "Viscous Force." Viscous Force - Schlumberger Oilfield Glossary, Schlumberger Oilfield Glossary, www.glossary.oilfield.slb.com/en/Terms/v/viscous_force.aspx.

[16] Nakayama, Y. Introduction to Fluid Mechanics. Butterworth-Heinemann, an Imprint of Elsevier, 1999.

[17] Lautrup, Benny. "Creeping Flow." Physics of Continuous Matter, The Niels Bohr Institute, www.cns.gatech.edu/~predrag/GTcourses/PHYS-4421-04/lautrup/7.7/creep.pdf.

[18] Jenson, V. G. "Viscous flow round a sphere at low Reynolds numbers (< 40)." Proceedings of the Royal Society of London. Series A. Mathematical and Physical Sciences 249.1258 (1959): 346-366.

[19] Nakayama, Y. Introduction to Fluid Mechanics. Butterworth-Heinemann, an Imprint of Elsevier, 1999.

[20] Nakayama, Y. Introduction to Fluid Mechanics. Butterworth-Heinemann, an Imprint of Elsevier, 1999.

The horizontal components of both forces act to resist flow. Here, that of τ (friction drag) is $\tau \sin\theta$, and that of p (form drag) is $p\cos\theta$.

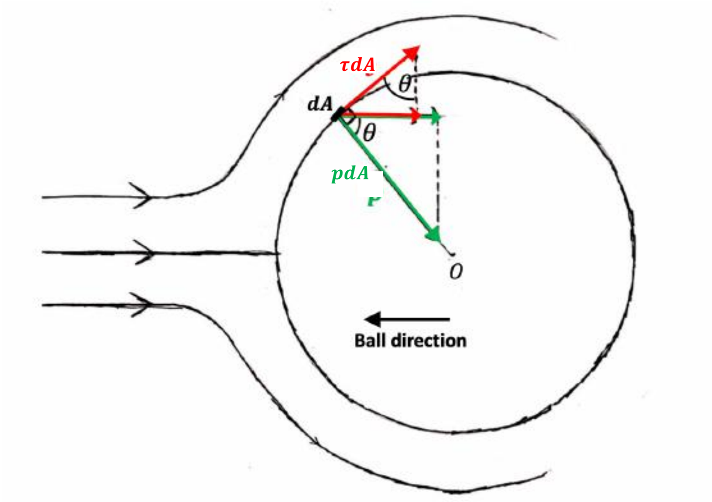

Figure 4 – Drag Force Components

Integrating these across all surface elements results in the total force produced from them[21]:

$$F_{friction} = \int_0^A \tau \sin\theta \, dA \quad (10)$$

$$F_{pressure} = \int_0^A p \cos\theta \, dA \quad (11)$$

Under conditions of Stokes flow around a sphere of radius r_0 moving with velocity v, the solutions are[22]:

$$F_{friction} = 4\pi\eta r_0 v \quad (12)$$

$$F_{pressure} = 2\pi\eta r_0 v \quad (13)$$

$$F_{drag} = F_{friction} + F_{pressure} = 6\pi\eta r_0 v \quad (14)$$

Equation (6) equals:

$$6\pi\eta r_0 v = \frac{4}{3}\pi {r_0}^3 g(\rho_{sphere} - \rho_{fluid}) \quad (15)$$

$$6\pi\eta v = \frac{4}{3}\pi {r_0}^2 g(\rho_{sphere} - \rho_{fluid}) \quad (16)$$

[21] Nakayama, Y. Introduction to Fluid Mechanics. Butterworth-Heinemann, an Imprint of Elsevier, 1999.
[22] "SIO 217D: Atmospheric and Climate Sciences IV: Atmospheric Chemistry." *:: SCRIPPS INSTITUTION OF OCEANOGRAPHY : UC SAN DIEGO ::*aerosols.ucsd.edu/sio217dwin14.html.

2.4. Navier-Stokes Equations

The Navier-Stokes equations are a set of partial differential equations that describe the flow of incompressible fluids, essentially represent Newton's second law but for fluids. These are applied to laminar flow between parallel surfaces. The equation, for direction *x* in a 1-dimensional flow, is[23]:

$$\rho\left(\frac{\partial u}{\partial t}+u\frac{\partial u}{\partial x}+v\frac{\partial u}{\partial y}\right)=\rho X-\frac{\partial p}{\partial x}+\eta\left(\frac{\partial^2 u}{\partial x^2}+\frac{\partial^2 u}{\partial y^2}\right) \tag{17}$$

Where *u* is the velocity in the x-direction, *v* is the velocity in the y-direction, *p* is the pressure, and X is the acceleration in the x-direction. In one-dimensional flow between parallel surfaces (in direction *x*) that is steady and uniform (velocity constant with displacement and time):

- $\frac{\partial u}{\partial t}=0$ (velocity is constant)
- $\frac{\partial u}{\partial x}=0$ (velocity does not vary with displacement in *x*)
- $v=0$ (no flow velocity in *y*)
- $X=0$ (no body force, and acceleration, in *x*)

Thus:

$$\eta\frac{\partial^2 u}{\partial y^2}=\frac{dp}{dx} \tag{18}$$

Integrating both sides of this equation with respect to y twice results in an expression for the velocity:

$$\eta\int\frac{\partial u}{\partial y}\partial y=\frac{dp}{dx}\int y\,dy+\int c_1\ dy \tag{19}$$

$$u=\left(\frac{1}{2\eta}\right)\left(\frac{dp}{dx}\right)y^2+c_1y+\ c_2 \tag{20}$$

Applying the no-slip condition for parallel surfaces separated by a distance *h*, *u = 0* at *y = 0* and *y = h*. The equation simplifies to (see **Appendix 10.2** for derivation):

[23] Nakayama, Y. Introduction to Fluid Mechanics. Butterworth-Heinemann, an Imprint of Elsevier, 1999.

$$u = \left(\frac{1}{2\eta}\right)\left(\frac{dp}{dx}\right)y(y-h) \tag{21}$$

The velocity *u* varies parabolically with displacement *y*.

2.5. Modelling the Wall Effect

2.5.1. Model

Consider a sphere of radius r_0 moving horizontally through unbounded fluid of viscosity μ at velocity v ms^{-1}. The total drag force experienced is $6\pi\eta r_0 v$. When the sphere travels through a fluid bounded in a cylinder of radius R at velocity v ms^{-1}, $F_{drag} = -kv$, where k is the drag coefficient. In this case, $k > 6\pi\eta r_0$ due to an increase in velocity gradient at the sphere, as a parabolic variation of velocity with is formed. This results in increased shear stress, increased skin friction drag and increased drag force.

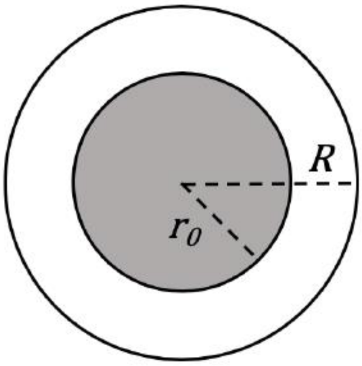

Figure 5 – Cross-sectional depiction of radii.

In the sphere's reference frame, the fluid moves at velocity v ms^{-1} in the opposite direction. Since v is constant, it must be equal at all points in the flow; therefore, the velocity of fluid immediately adjacent to the sphere is equal to the velocity of fluid ahead of the sphere. Hence, in a parabolic velocity distribution, the maximum (centreline) velocity is also *v*.

It is also known that the zeroes of this distribution lie at $y = 0$ and $y = R - r$, where r is the radius of any cross-sectional circle in the sphere, ranging from 0 to r_0.

If the velocity at any point on the distribution is *u*, then:

$$u = ay\big(y - (R - r)\big) \tag{22}$$

Where *a* is an unknown scale factor. First, *a* is determined, as this allows the value of *du/dy* at *y* = *R* – *r* to be determined in terms of *r*, using which the shear stress and frictional drag can be computed.

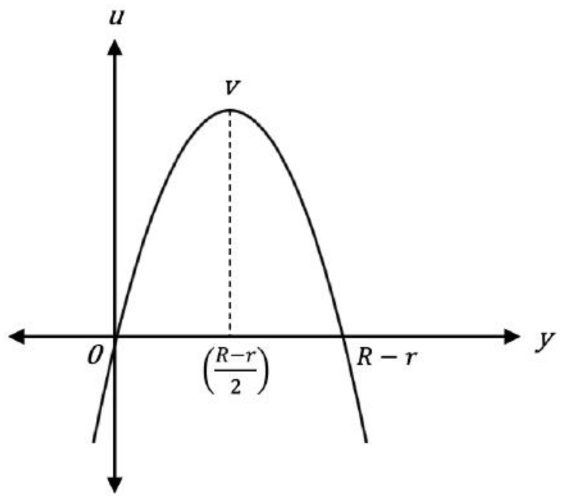

Figure 6 – Parabolic velocity distribution

When $y = \left(\frac{R-r}{2}\right)$, $u = v$:

$$v = -a\left(\frac{R-r}{2}\right)\left(\frac{R-r}{2}\right) \tag{23}$$

$$a = \frac{-4v}{(R-r)^2} \tag{24}$$

The velocity distribution function is:

$$u = \frac{-4v}{(R-r)^2}y\big(y - (R - r)\big) \tag{25}$$

The velocity gradient is:

$$\frac{du}{dy} = \frac{-4v}{(R-r)^2}\big(2y - (R - r)\big) \tag{26}$$

At $y = R - r,$ the surface of the sphere:

$$\frac{du}{dy} = \frac{-4v}{(R-r)^2}\big(2(R-r) - (R - r)\big) = \frac{-4v}{R-r} \tag{27}$$

The shear stress, as per equation (8), is:

$$\tau = \frac{-4\eta v}{R - r} \tag{28}$$

As indicated by equation (10), the component of the shear stress contributing to drag is equal to $\tau \sin\theta$.

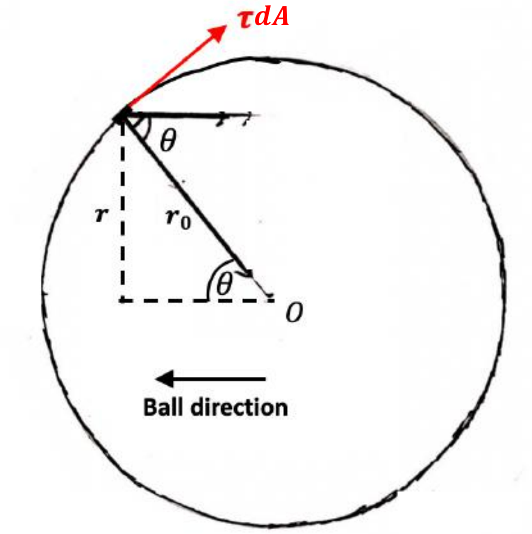

Figure 7 – Shear Stress at arbitrary value of r

At a value of *r* between the given range:

$$\sin\theta = \frac{r}{r_0} \tag{29}$$

$$\tau \sin\theta = \frac{-4\eta v}{R - r} \times \frac{r}{r_0} \tag{30}$$

To calculate the drag force generated by the increased shear stress caused by the wall, equation (30) must be integrated with respect to ***dA***. In cylindrical coordinates, ***dA*** = ***r dr dϕ***. Hence:

$$F_{friction(wall)} = \int_0^A \tau \sin\theta \, dA = \frac{-4\eta v}{r_0} \int_0^{2\pi} \int_0^{r_0} \frac{r^2}{R - r} \, dr \, d\phi \tag{31}$$

Upon integrating using *u-substitution* (see **Appendix 10.3**), the following is obtained as the magnitude (absolute value) of this force:

$$F_{friction(wall)} = \frac{8\pi\eta v}{r_0}\left[R^2 \ln\left|\frac{R}{R - r_0}\right| - Rr_0 - \frac{r_0^2}{2}\right] \tag{32}$$

Hence, the total drag force equates to $F_{friction(wall)} + F_{unbounded}$:

How does the relative radius of a sphere affect the relative drag force it experiences in a bounded medium?

$$F_{Drag(TotalWall)} = \frac{8\pi\eta v}{r_0}\left[R^2 \ln\left|\frac{R}{R-r_0}\right| - Rr_0 - \frac{r_0^2}{2}\right] + 6\pi\eta r_0 v \quad (33)$$

Dividing the contents of the bracket by r_0^2 allows factorization as follows:

$$F_{Drag(TotalWall)} = 2\pi\eta v r_0 \left[\frac{4R^2}{r_0^2}\ln\left|\frac{R}{R-r_0}\right| - \frac{4R}{r_0} + 1\right] \quad (34)$$

The numerator and denominator within the logarithm are divided by R;

$$F_{Drag(TotalWall)} = 2\pi\eta v r_0 \left[\frac{4R^2}{r_0^2}\ln\left|\frac{1}{1-\frac{r_0}{R}}\right| - \frac{4R}{r_0} + 1\right] \quad (35)$$

The increase in drag force is computed by considering the ratio of the total drag in a wall to the total drag in an unbounded medium.

$$\frac{F_{Drag(TotalWall)}}{F_{Drag(TotalUnbounded)}} = \frac{F_W}{F_\infty} = \frac{2\pi\eta v r_0 \left[\frac{4R^2}{r_0^2}\ln\left|\frac{1}{1-\frac{r_0}{R}}\right| - \frac{4R}{r_0} + 1\right]}{6\pi\mu v r_0} \quad (36)$$

$$\frac{F_W}{F_\infty} = \frac{1}{3}\left[\frac{4R^2}{r_0^2}\ln\left|\frac{1}{1-\frac{r_0}{R}}\right| - \frac{4R}{r_0} + 1\right] = \frac{4R^2}{3r_0^2}\ln\left|\frac{1}{1-\frac{r_0}{R}}\right| - \frac{4R}{3r_0} + \frac{1}{3} \quad (37)$$

Defining the variable in the equation to be $c = \frac{r_0}{R}$, where $r_0 < R$, in the range $0 < \lambda < 1$, and the output as relative drag $\left(k_{drag} = \frac{F_W}{F_\infty}\right)$, equation (37) is re-expressed:

$$k_{drag} = \frac{F_W}{F_\infty} = \frac{4}{3c^2}\ln\left|\frac{1}{1-c}\right| - \frac{4}{3c} + \frac{1}{3} \quad (38)$$

The ratio examined, in this model, is not directly dependent on the values of r_0 and R, but on their ratio $c = \frac{r_0}{R}$.

When plotted, while undefined at $c = 0$ (indicative of unbounded medium), the limit of the function at this value is 1, which adheres to the expectation that $\frac{F_\infty}{F_\infty} = 1$. Furthermore, the expectation at $c = 1$ would be that the drag force is infinite, as the radius of the sphere and cylinder are equal, resulting in infinite velocity gradient. This is the case here, as at $c = 1$, a vertical asymptote is found.

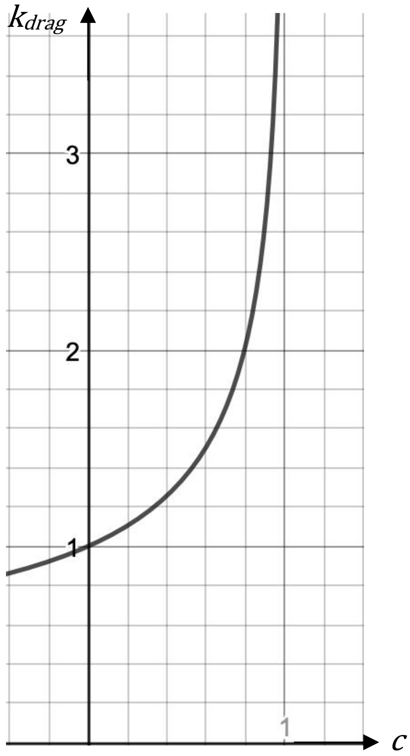

Graph 1 – Theoretical Function for Wall Effect (Equation 38)

In a falling sphere viscometer, the force remains constant as the effective weight (*weight – buoyant force)* is constant regardless of the wall. However, an increased drag force means that the terminal velocity attained is lower due to greater resistance with the same increase in velocity.

2.5.2. Assumptions

This model is valid under the following **assumptions**:

- The wall effect on drag only occurs due to increase of frictional drag, not pressure drag as well.
- The velocity gradient in an unbounded medium is equivalent to zero (increase in velocity is spread over infinite distance from the sphere).
- All flow is strictly laminar.

How does the relative radius of a sphere affect the relative drag force it experiences in a bounded medium?

3. VARIABLES

3.1. Independent Variable

As per formulated equation (38), the independent variable in the investigation is the relative radius of the sphere (ball) $\left(c = \frac{r_0}{R}\right)$. Since a single tube of constant diameter is used, this is varied by varying the radius of ball bearings r_0. Both r_0 *and* R were measured using a Vernier Calliper (**Appendix 10.4**). Uncertainty calculations for *c* are in **Appendix 10.7.**

Ball Radius $r_0 \pm 0.01cm$	**Tube Radius** $R \pm 0.01cm$	**Relative Radius** $c = r_0/R$	**Uncertainty in Relative Radius** Δc
0.15	1.25	0.120	0.009
0.32	1.25	0.254	0.010
0.48	1.25	0.381	0.011
0.64	1.25	0.508	0.012
0.79	1.25	0.635	0.013
0.95	1.25	0.762	0.014

Table 1 – Independent Variable Values

3.2. Dependent Variable

The ratio of the drag force in a bounded medium to that in an unbounded medium (F_W/F_∞) is the unitless dependent variable, "relative drag" (k_{drag}). When terminal velocity (v_t) is reached and $\Sigma F = 0$, measured viscosity (η) is solved for. Equation (16) is rearranged for this:

$$\eta = \frac{2gr_0^2\left(\rho_{sphere} - \rho_{liquid}\right)}{9v_t} \tag{39}$$

Since $F \propto \eta$ in Stokes' Law, the measured viscosity is increased by the same factor (k_{drag}). Hence: $k_{drag} = \frac{\eta}{\eta_\infty}$, the ratio of η to the viscosity that would be measured in an unbounded medium (η_∞).

η is determined by calculating the terminal velocity, by tracking the position *y* of the sphere as it falls η_∞ is determined using non-linear extrapolation of η to $c = 0$.

3.3. Controlled Variables

Controlled Variable	Description	Value
Viscosity of Fluid (η)	Affects the experienced drag; controlled by using the same fluid glycerine at the same concentration.	*Experimentally Determined*
Temperature	Affects density and viscosity of fluid, and hence the drag and buoyant forces experienced. Controlled using thermometer and thermostat (6 hours equilibration time).	(25.0 ± 0.25)℃
Density of Fluid (ρ_{liquid})	Affects the buoyant force drag; controlled by using the same fluid glycerine at the same concentration. Due to the adhesive nature of the fluid, determining the volume for density calculations was subject to inaccuracy. Hence, literature values[24] were used. The given uncertainty is a sum of the interpolated value of the density at 25.0℃ *and* half the difference of the values $\pm$0.25℃ (**Appendix 10.5**).	(1017.38 ± 0.63) kgm^{-3}
Rotational Energy	Rotational motion impacts drag – this results in motion of fluid on the surface of the ball, impacting the velocity gradient. Using the release mechanism minimizes any such effects.	*0 J*

[24] Glycerine Producers' Association. Physical properties of glycerine and its solutions. Glycerine Producers' Association, 1963.

Sphere Density (ρ_{sphere})	This also affect the buoyant force. Although accountable if measurements of each ball type are used, due to the minute mass of the smaller ball, this is considered constant by using the same material for each – AISI 52100 steel (American Iron & Steel Institute). The density is determined using the largest ball (known volume = (3.59 $\pm$ 0.03) cm^3, measured mass = (28.04 $\pm$ 0.01) g). This value is exactly that provided by the manufacturer[25].	(7.81 ± 0.07) gcm^{-3} $=$ (7810 ± 70) kgm^{-3}
Minimum height of region of fall analysed	The *end effect* arises from the proximity of the bottom of the tube to the falling sphere. This is negligible if the distance to the end is lesser than the radius of the tube[26].	$> 1.25cm$
Horizontal distance of camera from tube	*Parallax* in video analysis can distort velocity measurements. the camera is positioned as far away as possible without compromising the clarity of the balls, which also impacts the accuracy of video analysis.	$(107.10 \pm 0.05)\ cm$

[25] *AZoM. "AISI 52100 Alloy Steel (UNS G52986)." AZoM.com, AZoM, 26 Sept. 2012, www.azom.com/article.aspx?ArticleID=6704.*

[26] Tanner, R. I. "End effects in falling-ball viscometry." *Journal of Fluid Mechanics* 17.2 (1963): 161-170.

4. EXPERIMENTAL DESIGN

4.1. Apparatus

APPARATUS	
Vernier Calliper ($\pm 0.01cm$)	Tube (Radius = 1.25cm $\pm 0.01cm$)
Chrome Steel Ball Bearings (AISI 52100)[27] of Radii 0.15cm, 0.32cm, 0.48cm, 0.64cm, 0.79cm, 0.95cm ($\pm 0.01cm$).	
Glycerine Fluid (100% Glycerol)	Top Pan Balance ($\pm 0.01g$)
Thermometer (± 0.25°C)	Video Camera with 240fps frame rate
Tripod Stand	Measuring Tape ($\pm 0.05cm$)
Iron Nail	$3 \times 9V$ Cells
Crocodile Connector Wires	Enamel-Coated Copper Wire
Bubble Wrap	Magnet (to remove ball bearings)

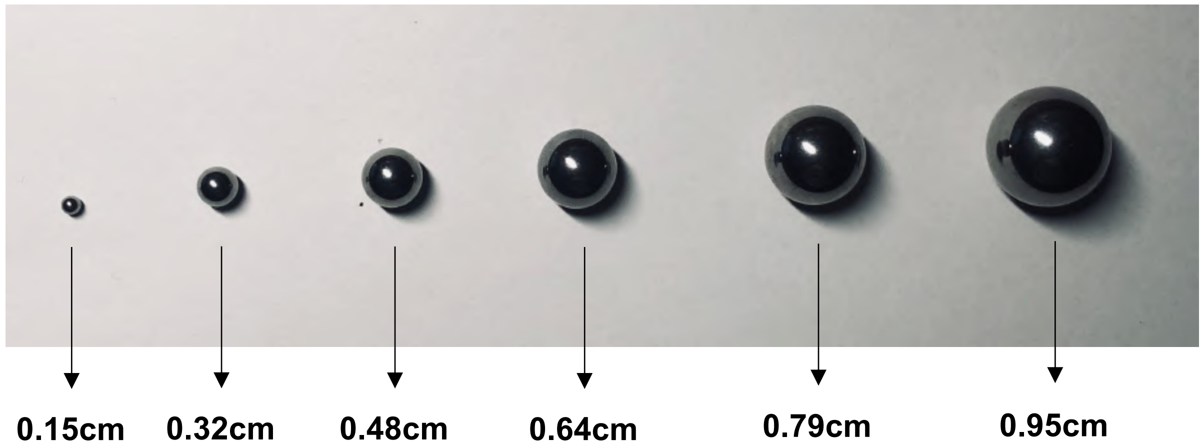

Figure 8 – Ball Bearings Used

[27] *AZoM. "AISI 52100 Alloy Steel (UNS G52986)." AZoM.com, AZoM, 26 Sept. 2012, www.azom.com/article.aspx?ArticleID=6704.*

4.2. Setup

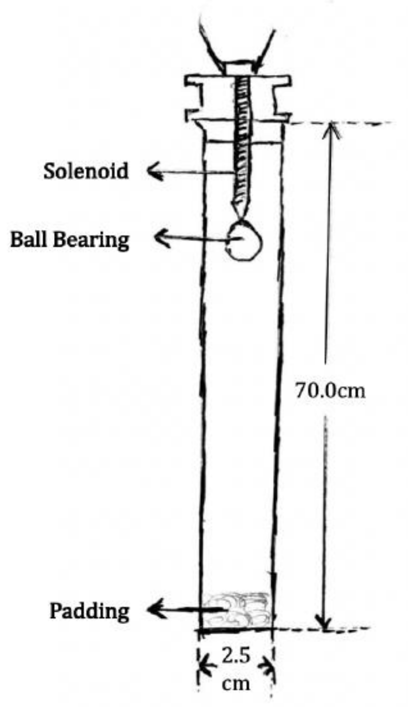

Figure 9 – Diagram of tube

- The chrome steel ball bearings fall through a tube of height 70.0cm. However, the height to which their motion is analysed is shorter than this. This is because the tube is easily pushed to disequilibrium. The bottom was inserted through a wide cardboard box, in order to ensure this does not happen, reducing this distance.

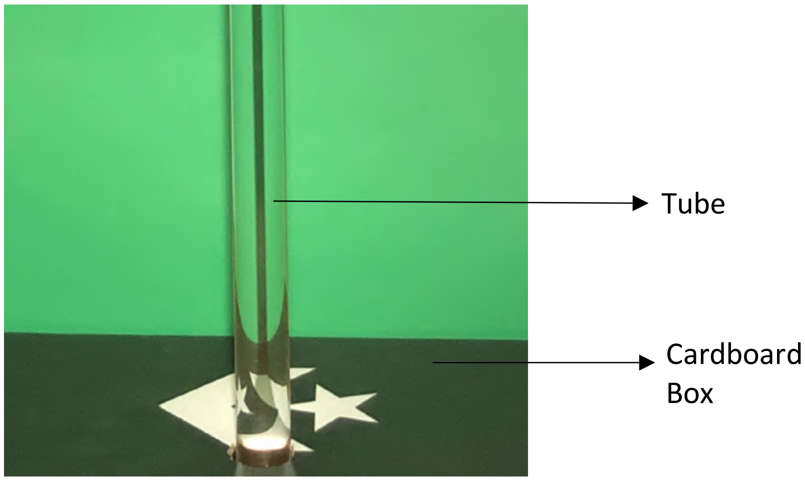

Figure 10 – Tube Passing Through Cardboard Box

- All measurements were taken using video analysis, conducted on the free software *Tracker*[28].

- **Glycerine** was selected due to its high viscosity. If maximum speed is considered (considering maximum possible Reynolds' number):

Quantity	Value
Maximum average speed ($c = 0.381$)	0.0901 ms^{-1}
Viscosity (η) at 25°C (interpolated from literature[29] (**Appendix 10.6**))	0.93013 Pas
Density at 25°C	1017.38 kg m^{-3}
Diameter of bearing	$0.0048 \times 2 = 0.0096m$

Table 2 – Reynolds' Formula Inputs

Inserting these values in equation (9), the Reynolds' number is computed:

$$\frac{0.0901ms^{-1} \times 1017.38\ kgm^3 \times (0.0250 - 0.0096)\ m}{0.9489\ Pa\ s} = 1.49$$

Though greater than 1, this is significantly lower than Re = 17, where flow separation occurs.[30]

- Ball bearings were dropped using a **release mechanism:** a solenoid made using an iron nail, connected to a 27-volt power supply and a switch. When turned on, the nail was magnetized, and the ball bearing was lifted and placed into the tube (filled with glycerine) – its position was within the fluid to avoid a change of medium and any change in rate of increase of drag. This rested on the tube. When demagnetized, the ball fell *straight*, *without rotation about a horizontal axis* and was released *stably*, which could not be achieved by hand.

---

[28] Brown, Douglas. Tracker Video Analysis and Modeling Tool. Vers. 5.1.3. Computer software. 2020. 2 Feb. 2020 <http://physlets.org/tracker/>.
[29] Glycerine Producers' Association. Physical properties of glycerine and its solutions. Glycerine Producers' Association, 1963.
[30] Jenson, V. G. "Viscous flow round a sphere at low Reynolds numbers (< 40)." Proceedings of the Royal Society of London. Series A. Mathematical and Physical Sciences 249.1258 (1959): 346-366.

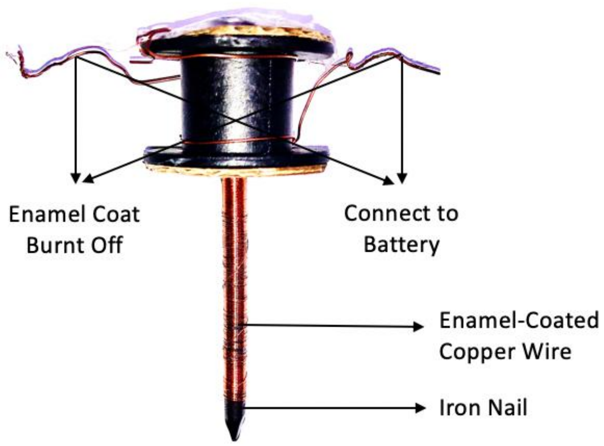

Figure 11 – Picture of Release Mechanism

4.3. Video Analysis – Parameters & Calibration

Parameter	Value
Distance from Tube *(D)*	$(107.10 \pm 0.05)\ cm$
Height of Camera Lens *(H)*	$(54.6 \pm 0.05)\ cm$
Video Frame Rate	30 fps

Table 3 – Video Analysis Parameters

In all analysis, the length was calibrated by setting a line crossing the tube, parallel to the aligned *x-axis*, equal to the diameter of the tube.

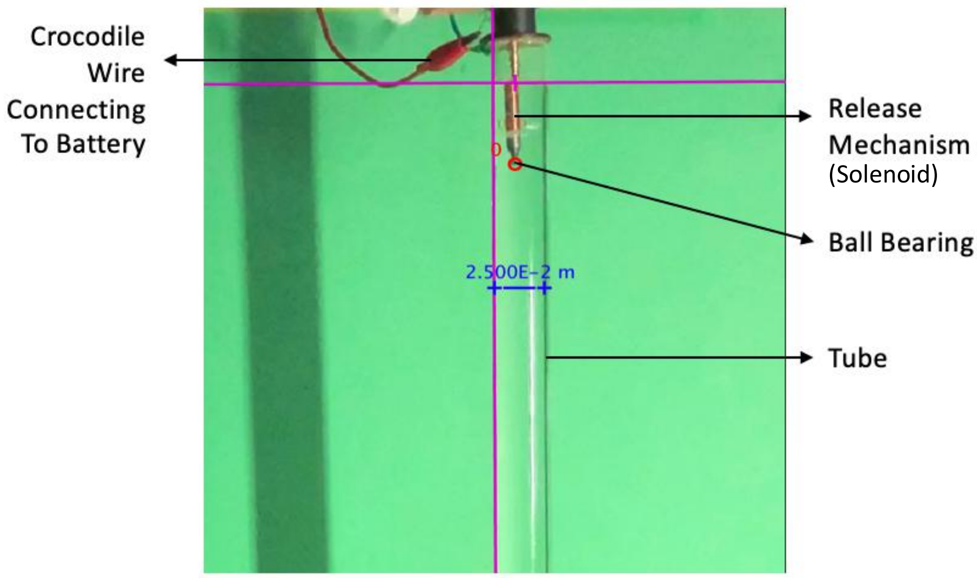

Figure 12 – Tube and Ball in Tracker Software

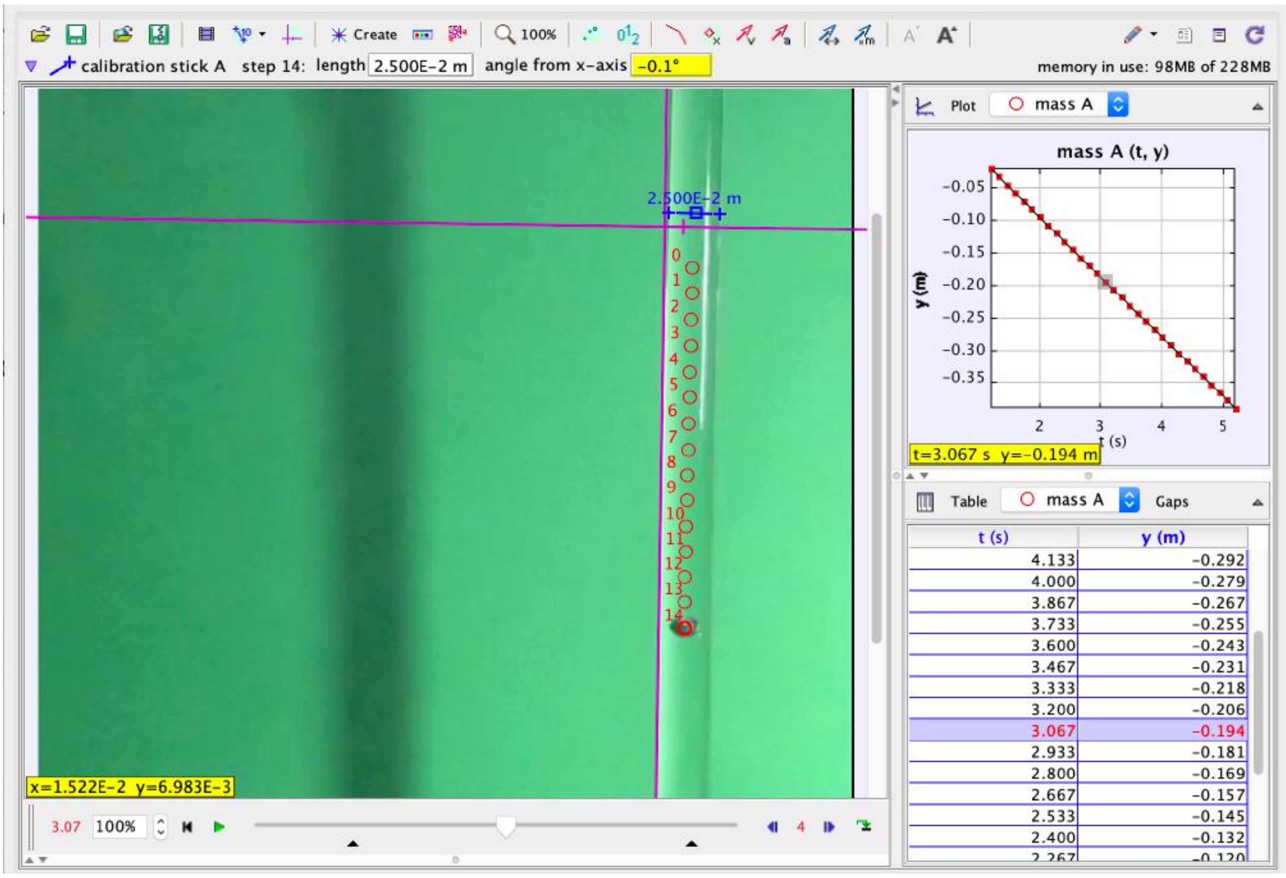

Figure 13 – Screenshot of Tracking (r_0 = 0.48cm)

4.4. Safety Considerations

- Care taken while handling all electric components to the release mechanism due to moderate voltage involved.
- Padding (bubble wrap) pushed to its bottom to reduce time taken for the momentum of the ball bearings to decrease to zero and hence impact force, due to tube's highly fragile nature.
- Tube passed though Cardboard Box (*Figure 10*) to increase stability by widening base, hence preventing falls.
- Mercury thermometer handled with extreme care.

5. DATA & ANALYSIS

5.1. Calculating Terminal Velocities

Terminal velocities (v_t) were found by considering the strongly linear portions of the graphs of vertical displacement (*y/m)* against time *(t/s)*, and calculating the gradients. The *coefficient of determination* (R^2 value) for all linear graphs was greater than 0.999, which strongly supports linearity of y variation and hence constant v_t.

Times were calculated by considering frame duration. Given a frame rate of 30fps, each frame was equivalent to $\frac{1}{30}s$. The distance was measured with an uncertainty based on the smallest pixel; however, due to other sources of uncertainty (e.g. parallax), this was not reflective of the overall uncertainty. An arbitrary number of decimal places (6) was hence used for determining statistical measures, which were used to define the decimal places of all mean velocities. 5 repeats were carried out for each value of c. Since only the magnitude of the terminal velocity is necessary for calculation, only absolute values are considered.

Relative Radius $c = r_0/R$	Terminal Velocity $(v_t)/\ ms^{-1}$					
	Trial 1	Trial 2	Trial 3	Trial 4	Trial 5	Mean
0.120	~~0.022047~~	0.026885	0.027085	0.027021	0.028870	0.027465
0.254	0.074734	0.072006	0.077554	0.072236	0.075312	0.074368
0.381	0.090000	0.089749	0.091344	0.090388	0.088981	0.090092
0.508	0.064392	0.065824	0.065836	0.064784	0.065995	0.065366
0.635	0.034252	0.033116	0.032083	0.033564	0.035510	0.033705
0.762	0.006301	0.006250	0.006112	0.006292	0.006063	0.006204

Table 4 – Raw Data of Terminal Velocities

The value struck through was considered anomalous due to significant deviation from other values. Hence, the mean and standard deviation for $c = 0.120$ were calculated using values from trial 2 to 5. Another observation that can be found in the given data is that the value of the velocity for $c = 0.762$ is far lower than any other value by an approximate factor of 5. This trend continues in an even more drastic fashion as viscosities and hence k_{drag} are calculated, and is evaluated in **Section 7** (Evaluation).

Since no accurate experimental measure of uncertainty exists, standard deviation was used. Percentage uncertainties were then calculated; since only 5 repeats were taken, the data was insufficient have an accurate measure of the standard deviation. Hence, the maximum fractional uncertainty found was considered for all values of c, and the absolute uncertainties were recalculated. These defined decimal places assigned.

Relative Radius $c = r_0/R$	**Uncertainty in Terminal Velocity** $(\Delta v_t)/ms^{-1}$	**Fractional Uncertainty in** $v_t \left(\frac{\Delta v_t}{v_t}\right)$	**MAX** $\frac{\Delta v_t}{v_t}$	**Recalculated** $\Delta v_t/ms^{-1}$	**Recalculated** $\Delta v_t/ms^{-1}$ **(rounded)**	**Mean Terminal Velocity** $(v_t)ms^{-1}$
0.120	0.00081	0.029646	0.037980	0.00104	0.0010	0.0275
0.254	0.00231	0.031029		0.00282	0.0028	0.0744
0.381	0.00087	0.009638		0.00342	0.0034	0.0901
0.508	0.00073	0.011121		0.00248	0.0025	0.0654
0.635	0.00128	0.037980		0.00128	0.0013	0.0337
0.762	0.00011	0.017587		0.00024	0.0002	0.0062

Table 5 – Uncertainties in terminal velocity

Correct to three significant figures (as per the mean v_t), fractional uncertainty is 0.0380 [3.80%].

5.2. Calculating Viscosity

Equation 41 is used to calculate viscosities, using the above mean velocities, values of r_0 present in table 1, and values of ρ_{sphere} and ρ_{fluid} from the table of controlled variables. Uncertainties are calculated as follows:

$$\frac{\Delta\eta}{\eta} = \frac{2\Delta r_0}{r_0} + \frac{\Delta v_t}{v_t} + \frac{\Delta(\rho_{sphere} - \rho_{fluid})}{\rho_{sphere} - \rho_{fluid}} + \frac{\Delta g}{g} \quad (40)$$

$$\rho_{sphere} - \rho_{fluid} = (7810 \pm 70)\ kgm^{-3} - (1015.67 \pm 0.61)\ kgm^{-3}$$
$$= (6794.33 \pm 70.61)\ kgm^{-3}$$

$$\Delta(\rho_{sphere} - \rho_{fluid}) = 70.61\ kgm^{-3}$$
$$\frac{\Delta(\rho_{sphere} - \rho_{fluid})}{\rho_{sphere} - \rho_{fluid}} = \frac{70.61}{6794.33} = 0.01039$$
$$\frac{\Delta v_t}{v_t} = 0.0380$$
$$2\Delta r_0 = 0.0002m$$

The value used for gravitational acceleration g is the constant 9.81 ms^{-2}, with no uncertainty.

Relative Radius $c = r_0/R$	**Ball Radius** r_0/m	**Fractional Uncertainty in** r_0 $\left(\frac{\Delta r_0}{r_0}\right)$	**Mean** v_t/ms^{-1}	**Viscosity** $\eta\ /Pas$	**Fractional Uncertainty in** η $\left(\frac{\Delta\eta}{\eta}\right)$	**Uncertainty in** η $(\Delta\eta/Pas)$
0.120	0.0015	0.067	0.0275	1.21	0.182	0.22
0.254	0.0032	0.031	0.0744	2.04	0.111	0.23
0.381	0.0048	0.021	0.0901	3.79	0.090	0.34
0.508	0.0064	0.016	0.0654	9.28	0.080	0.74
0.635	0.0079	0.013	0.0337	27.4	0.074	2.0
0.762	0.0095	0.011	0.0062	215	0.069	15

Table 6 – Calculated Viscosities and Uncertainties

5.3. Calculating the Viscosity Ratio

In order to calculate the relative drag $k_{drag} = \frac{F_W}{F_\infty} = \frac{\eta}{\eta_\infty}$, the value of η_∞ (viscosity measured in an unbounded medium) must be estimated. This is done by performing a non-linear extrapolation of data for viscosities, and estimating the value of viscosity when $c = 0$.

While there is no theoretical reference justifying an exponential fit of this data, this is chosen over high-order polynomial fitting because the predictable trend is one that clearly rises from a fixed value at $c = 0$ at a constantly increasing rate for $c < 1$. For polynomial fits, the gradient and value do not increase in the above region. Furthermore, this fit has lower complexity (fewer parameters) than high-order polynomials, reducing the sources of error.

Due to the large value of the calculated viscosity for $c = 0.762$, and hence large absolute error, it is discounted in the fitting of the data for extrapolation, as an uncertainty of 30 *Pas* allows for significant variation in the trendline that can be fitted. Furthermore, the application of this results in error greater than the smallest value of η itself.

The equation found (of the form $a + be^{kx}$) was:

$$\eta = 1.115276 + 0.07967223e^{9.131281c} \tag{41}$$

The R^2 value of this fit was 0.9999, and the standard error (*SE*) of points not directly lying on the curve (residuals) was 0.1544 *Pa s*. This value is the root mean square of the difference between the residuals and the curve, and is hence considered to be the uncertainty when extrapolated to $c = 0$. Hence:

$$\eta_\infty = 1.115276 + 0.07967223e^{9.131281(0)} = 1.115276 + 0.07967223$$
$$= (1.1949823 \pm 0.1544)\ Pa\ s$$
$$\Delta\eta_\infty = 0.1544\ Pa\ s$$

Given a calculation of all other viscosities with $\mu < 10$ to two decimal places, this is approximated to $(1.19 \pm 0.15)\ Pa\ s$.

The fractional uncertainty in η_∞ is:

$$\frac{\Delta\eta_\infty}{\eta_\infty} = \frac{0.15}{1.19} \approx 0.13$$

The total uncertainty in $k_{drag} = \frac{\eta}{\eta_\infty}$ is:

$$\frac{\left(\frac{\Delta\eta}{\eta_\infty}\right)}{\left(\frac{\eta}{\eta_\infty}\right)} = \frac{\Delta\eta_\infty}{\eta_\infty} + \frac{\Delta\eta}{\eta} \tag{42}$$

5.4. Processed Data

Data for the variation of k_{drag} with c is presented in *Table 6*.

Relative Radius $c = r_0/R$	**Viscosity $(\eta)/Pa\ s$**	**Viscosity in Unbounded Medium $(\eta_\infty)/Pa\ s$**	**Relative Drag (k_{drag})**	**Fractional Uncertainty in Relative Drag $\left(\frac{\Delta k_{drag}}{k_{drag}}\right)$**	**Uncertainty in Relative Drag (Δk_{drag})**
0.120	1.21	1.19	1.02	**0.312**	0.317
0.254	2.04	1.19	1.71	**0.241**	0.413
0.381	3.79	1.19	3.18	**0.220**	0.701
0.508	9.28	1.19	7.80	**0.210**	1.64
0.635	27.4	1.19	23.0	**0.204**	4.70
0.762	215	1.19	181	**0.199**	36.0

Table 7 – Processed Data

This data is graphed in graphs *2a* and *2b* (due to difference in orders of magnitude, two graphs are presented to ensure clarity.

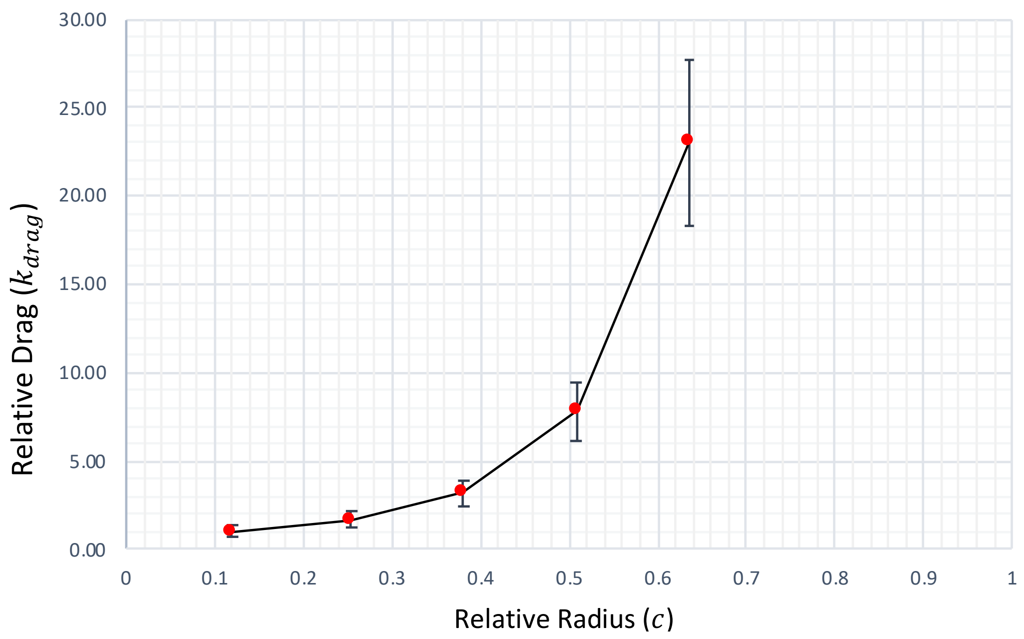

Graph 2a – *Excluding* $c = 0.762$

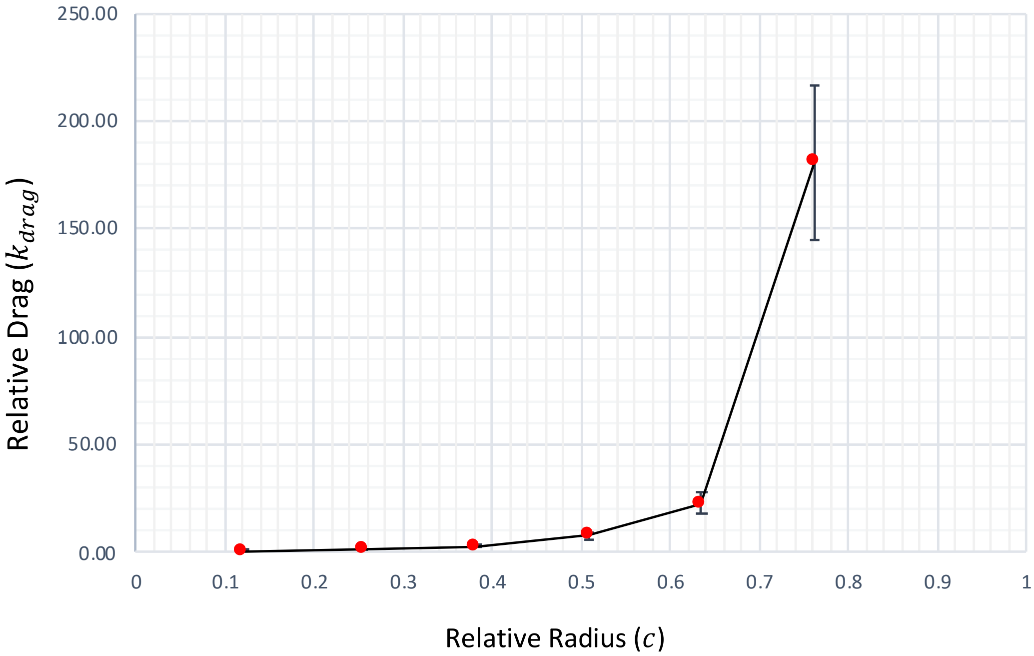

***Graph 2b** – Including* $c = 0.762$

Curve fitting has not been applied due to the lack of theory supporting an exponential or power function model of this data, and the inability to fit as per equation (38) on Microsoft Excel. As seen in Graph 2a and 2b, the relative drag increases as c increases, at an increasing rate.

5.5. Comparison with Theoretical Model

Uncertainties for the model are derived and calculated in **Appendix 10.8**.

The difference to the theoretical model is the experimental relative drag minus the theoretical relative drag: $\boldsymbol{E = k_{drag}(exp) - k_{drag}(calc)}$. The uncertainty in $\boldsymbol{E}$ is $\Delta \boldsymbol{E}$

Relative Radius $c = r_0/R$	**Theoretical Relative Drag (k_{drag}(calc))**	**Uncertainty in k_{drag}(calc) (Δk_{drag}(calc))**	**Experimental Relative Drag (k_{drag} (exp))**	**Uncertainty in k_{drag}(exp) (Δk_{drag}(exp))**	**Difference to Theoretical Model *(E)***	**Uncertainty in E (ΔE)**
0.12	1.06	9.55	1.02	0.317	-0.04	9.87
0.254	1.14	1.48	1.71	0.413	0.57	1.90
0.381	1.24	0.62	3.18	0.701	1.94	1.32
0.508	1.37	0.36	7.8	1.64	6.43	2.00
0.635	1.57	0.25	23	4.7	21.43	4.95
0.762	1.88	0.20	181	36	179.12	36.20

Table 8 – Theoretical Comparison including Error

The discrepancies are massive, far beyond the uncertainties permitted by the theoretical and experimental errors, and do not show any obvious quantitative trend. Due to this scale, theoretical and experimental values cannot be clearly represented on the same graph. Instead, $\ln(E)$ was plotted against c instead. The exponential curve for $\boldsymbol{E = k_{drag}(exp) - k_{drag}(calc)}$ was chosen purely due to its goodness of fit ($R^2 = 0.9831$). It is unclear whether the negative difference for is $c = 0.12$ is anomalous or not, due to the singular occurrence. Nonetheless, due to the single occurrence, it is ignored.

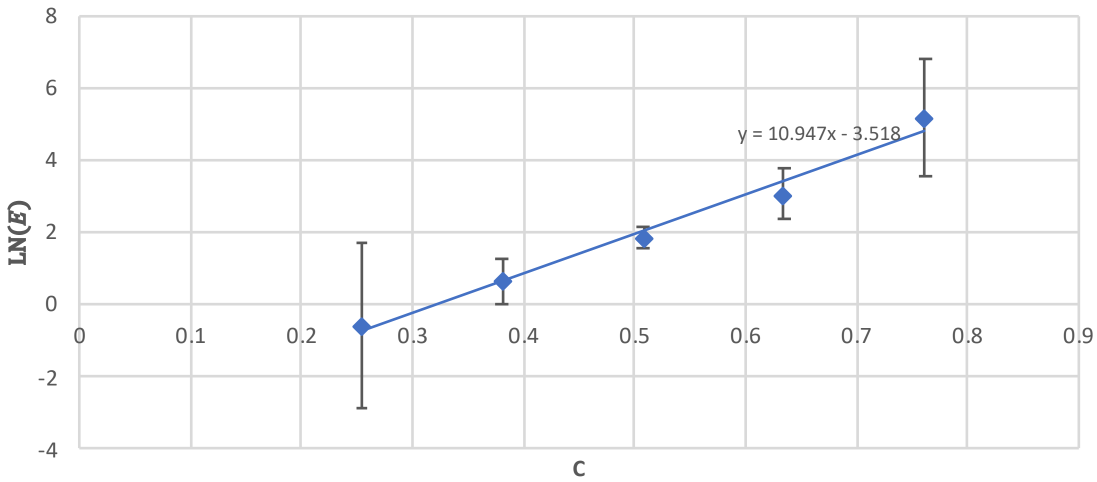

Graph 3 – Error versus Theory; ln(E) against c

$$\ln(E) = 11.0c - 3.52 \tag{43}$$

$$E = e^{-3.52} \times e^{11.0c} \tag{44}$$

6. CONCLUSION

Reconsidering the research question **"How does the relative radius of a sphere affect the relative drag force it experiences in a bounded medium?"**, it has been found that the relative drag (k_{drag}) increases, at an increasing rate, in the range $0 < c = \frac{r_0}{R} < 1$. This qualitatively agrees with theoretical predictions.

7. EVALUATION

Quantitatively, Equation (38) underestimates the experimental magnitude of the wall effect. It is not fully clear whether the error arises from experimental inaccuracy, theoretical inaccuracy, or some combination of both. To interpret this, literature data[31] for glycerine at the same temperature is analysed and compared with the data generated by the experiment. A tabulated form of the data in *Graph 3* was not provided by the authors. 5 arbitrary points were selected based on clarity, and straight lines parallel to the axes were used to determine their coordinates.

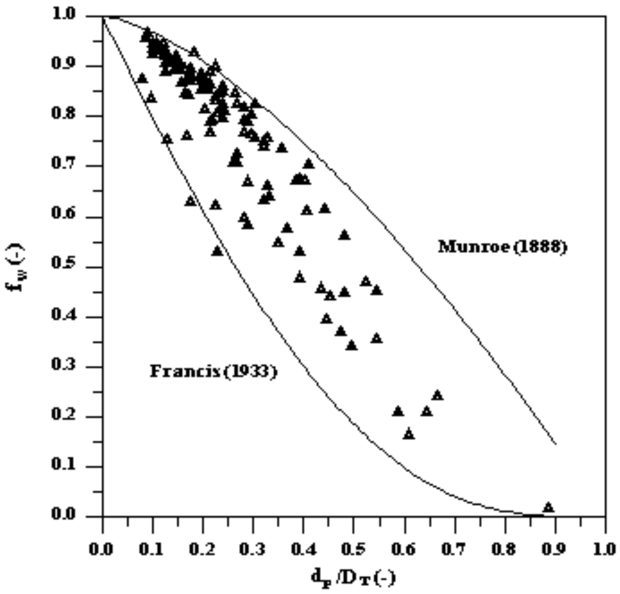

Graph 4 – Data from Ataíde (et al)[32]

The relative drag defined here was based on the terminal velocity ratio ($f_w = \frac{v_W}{v_\infty}$). Hence: $\boldsymbol{k_{drag}} = \frac{\boldsymbol{1}}{\boldsymbol{f_w}}$. No uncertainty is defined, and the values are assumed to be means due to single data points being present.

[31] Ataíde, C. H., F. A. R. Pereira, and M. A. S. Barrozo. "Wall effects on the terminal velocity of spherical particles in Newtonian and non-Newtonian fluids." Brazilian Journal of Chemical Engineering 16.4 (1999): 387-394.

[32] Ataíde, C. H., F. A. R. Pereira, and M. A. S. Barrozo. "Wall effects on the terminal velocity of spherical particles in Newtonian and non-Newtonian fluids." Brazilian Journal of Chemical Engineering 16.4 (1999): 387-394.

Relative Radius $c = r_0/R$	**Terminal Velocity Ratio ("f_w")**	**Relative Drag (k_{drag})**
0.095	0.835	1.20
0.167	0.76	1.32
0.390	0.477	2.10
0.496	0.339	2.95
0.606	0.165	6.06

Table 9 – Data Points from Graph 3

Fitting this data to a best-fit exponential curve (chosen for high R^2 value = 0.9974);

$$y = 1.206821 + 0.024637e^{8.711468x} \tag{45}$$

This is used to generate data for the conducted experiment's values for c and compared with both theoretical and experimental data (from Table 8).

Relative Radius $c = r_0/R$	**Literature Relative Drag (k_{drag}(lit))**	**Theoretical Relative Drag (k_{drag}(calc))**	**Experimental Relative Drag (k_{drag}(exp))**
0.12	1.28	1.06	1.02
0.254	1.43	1.14	1.71
0.381	1.89	1.24	3.18
0.508	3.26	1.37	7.8
0.635	7.43	1.57	23
0.762	20.0	1.88	181

Table 10 – Literature Estimates of k_{drag}

Generally, literature values under-predict the values for experimental k_{drag} measurements too, but, excluding the value for $c = 0.762$, these deviate on the same order of magnitude as the experimental data. However, considering the great variation in f_w on Graph 3 (vertically), the literature data has a high variance, and the data points are too close together to accurately estimate this. The experimental data can therefore be considered fairly consistent with literature.

The theoretical underestimation drastically increases with c. When $c = 0.762$, the data is likely erroneous and significantly deviating from literature because of the large r_0 and relative drag, which caused far lesser space between glass and ball. Direct contact between the two was not observed, which implies a radius-dependent fluid phenomenon. This could be due to the adhesive forces in boundary layers formed around the objects, that may exist between glass and ball directly in closed space. In addition, pressure drag may also increase if space between cylinder and fluid is smaller.

The inability to quantify experimental uncertainties directly in video analysis is a major issue. Parallax error cannot be analytically determined and the use of statistical measures of deviation is not wholly representative of the error allowed. Replacing video analysis with an array of photogate sensors would allow for far more accurate data, but these were unavailable. The release mechanism used has a significant impact for larger balls, which rested unstably and had to be carefully dropped. A mechanical mechanism where each size of ball is held tighter would likely lead to better results, which too was unavailable in this investigation.

Although the theoretically derived quantitative formula remains unjustified by experiment, one corrected for underestimation is derived by adding the error as a function of the relative radius c (Equation (44)) to this (Equation (38)).

$$k_{drag} = \frac{4}{3c^2}\ln\left|\frac{1}{1-c}\right| - \frac{4}{3c} + \frac{1}{3} + (e^{-3.52} \times e^{11.0c}) \qquad (46)$$

Overall, this agrees with experimental data that can be considered valid. Building on this understanding with studies recommended below can produce beneficial results for estimating the wall effect for biological or biotechnological applications.

8. FURTHER STUDIES

- Studies using multiple cylinder sizes and theoretical estimates for each could verify the contributions of boundary layers and any other non-linear effects.
- Non-linear analysis of the effects of the Reynolds' Number, and using several fluids of high viscosity would also enable extrapolation of the results to $Re = 0$ for increased accuracy of results.
- CFD (Computational Fluid Dynamics) simulations can be used to study the effect of the higher than one Reynolds numbers on the flow, and any impact on the drag force experienced. This could allow observational analysis of these non-linear effects.

9. BIBLIOGRAPHY

Ataíde, C. H., F. A. R. Pereira, and M. A. S. Barrozo. "Wall effects on the terminal velocity of spherical particles in Newtonian and non-Newtonian fluids." *Brazilian Journal of Chemical Engineering* 16.4 (1999): 387-394.

AZoM. "AISI 52100 Alloy Steel (UNS G52986)." *AZoM.com*, AZoM, 26 Sept. 2012, www.azom.com/article.aspx?ArticleID=6704.

Bonk, Ryan. "Buoyancy." *The Physics of Viking Ships*, University of Alaska, Fairbanks, ffden-2.phys.uaf.edu/webproj/212_spring_2017/Ryan_Bonk/purtyWebProj/vikingSlide1.html.

Brennen, C.E. *Internet Book on Fluid Mechanics*. Dankat Publishing, 2016.

Brown, Douglas. Tracker Video Analysis and Modeling Tool. Vers. 5.1.3. Computer software. 2020. 2 Feb. 2020 <http://physlets.org/tracker/>.

Cimbala, John M. "What Is Fluid Mechanics?" *Fluid Mechanics Electronic Learning Supplement*, Pennsylvania State University, www.me.psu.edu/cimbala/Learning/Fluid/Introductory/what_is_fluid_mechanics.htm.

Clift, Roland, John R. Grace, and Martin E. Weber. *Bubbles, drops, and particles.* Courier Corporation, 2005.

d'Alembert, Jean-Baptiste le Rond. "Force of inertia." The Encyclopedia of Diderot & d'Alembert Collaborative Translation Project. Translated by John S.D. Glaus. Ann Arbor: *Michigan Publishing, University of Michigan Library, 2006*. Web. [fill in today's date in the form 18 Apr. 2009 and remove square brackets]. <http://hdl.handle.net/2027/spo.did2222.0000.714>. Trans. of "Force d'inertie," Encyclopédie ou Dictionnaire

Fowler, Michael. “Dropping the Ball (Slowly).” Stokes' Law, University of Virginia, galileo.phys.virginia.edu/classes/152.mf1i.spring02/Stokes_Law.htm.

Francis, Alfred W. "Wall effect in falling sphere method for viscosity." *Physics 4.11* (1933): 403-406.

Glycerine Producers' Association. *Physical properties of glycerine and its solutions. Glycerine Producers' Association*, 1963.

Jenson, V. G. "Viscous flow round a sphere at low Reynolds numbers (< 40)." Proceedings of the Royal Society of London. *Series A. Mathematical and Physical Sciences* 249.1258 (1959): 346-366.

Nakayama, Y. Introduction to Fluid Mechanics. *Butterworth-Heinemann, an Imprint of Elsevier*, 1999.

Nave, R. *Surface Tension*, HyperPhysics, hyperphysics.phy-astr.gsu.edu/hbase/surten.html.

“SIO 217D: Atmospheric and Climate Sciences IV: Atmospheric Chemistry.” *:: SCRIPPS INSTITUTION OF OCEANOGRAPHY : UC SAN DIEGO ::*aerosols.ucsd.edu/sio217dwin14.html.

Song, Daoyun, Rakesh K. Gupta, and Rajendra P. Chhabra. "Wall effect on a spherical particle settling along the axis of cylindrical tubes filled with Carreau model fluids." *Proceedings of Comsol Conference, Boston*. 2011.

Tanner, R. I. "End effects in falling-ball viscometry." *Journal of Fluid Mechanics* 17.2 (1963): 161-170.

Schlumberger Oilfield Glossary. “Viscous Force.” Viscous Force – Schlumberger Oilfield Glossary, *Schlumberger Oilfield Glossary*, www.glossary.oilfield.slb.com/en/Terms/v/viscous_force.aspx.

10. APPENDIX

10.1. Researcher's Reflection Space

Both the difficulty and the breadth of things one must consider in narrowing down the research focus resulted in inhibitions in choosing Physics for the Extended Essay. However, these were diffused by how interesting potential topics were and the scope for my contributions. My initial interest was to understand the non-linear angular dependence of a pendulums period, frequency, and damping, through advanced math and experiment, because the validity of the small-angle approximation had always intrigued me. However, I was dissuaded from doing so due to the several other minute non-linearities that would have an impact. I was initially disheartened, but a discussion with my supervisors on alternatives assured me that I could continue with Physics.

I chose to consider a similar topic, in that it explores an effect otherwise approximated for simplicity, which introduced me to a new perspective on a familiar concept. I was drawn to drag and fluid dynamics due to their relation to the avenue of damping in the first topic. Initially, I thought about how there were two different formulae for drag under different conditions – one proportional to velocity and one to velocity squared. What would the relationship be in intermediate conditions? What other factors influence the validity of these equations? As I considered the means available to me to test any hypotheses, the most effective way to do so appeared to be motion through tubes. Here, the wall seemed to be likely to have major influence, and yet was never an effect I had been acquainted with. Hence, I chose to continue with the initial RQ: **"What is the effect of the proximity to the wall on drag?".**

Here, the options for experiment included CFD Simulations, Flow Analysis, Horizontal Motion of Fluid over a fixed object, or objects falling through the tube. I chose the last one due to the established efficacy and potential to further modify rather than just achieve. I made the following initial roadmap:

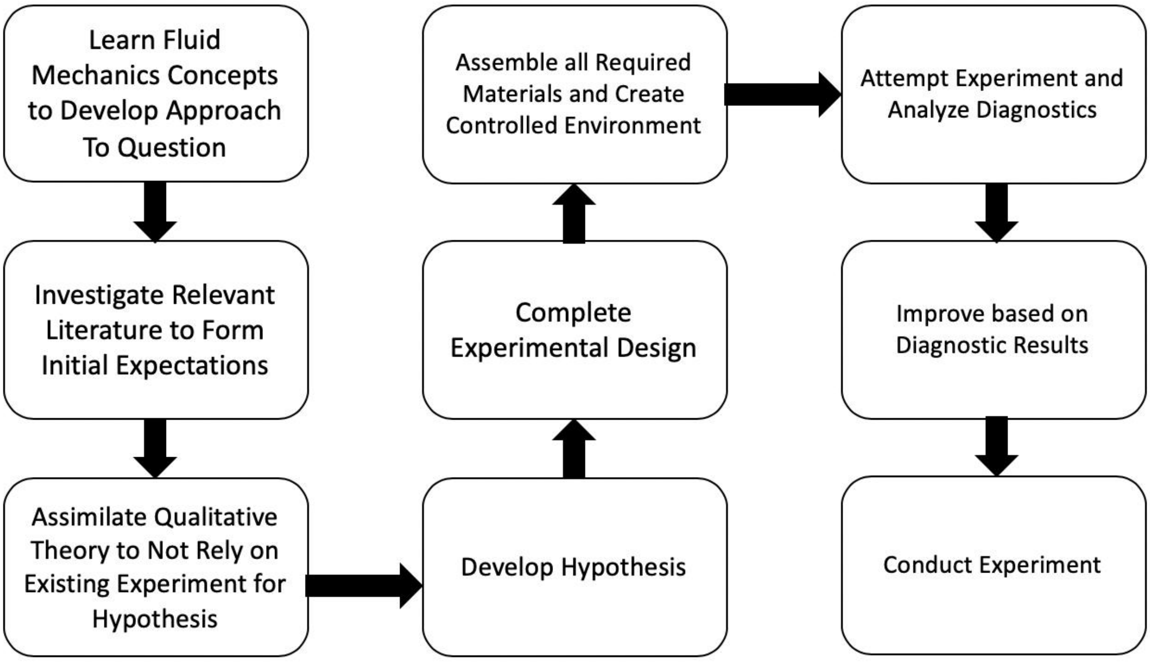

Figure 10.1.1 – Mind Map

Following data collection stages, analysis and evaluation would be performed, and subsequent drafts would be written after consultation with my supervisor.

Upon gaining an understanding of the work already done, I began articulating the variables in terms of relative radius and 'wall factor', which I redefined more intuitively as 'relative drag'. My intention was first to emphasize the fitting, statistical, and analytical aspects of the research. This allowed me to reframe the RQ as "**How does the relative radius of a sphere affect the relative drag force it experiences in a bounded medium?"**.

To this end, I wished to remove the effect of even the already low Reynolds' Number by conducting at different glycerin concentrations and approximating the 'wall factor' to Re = 0, and perhaps even correlate observations to those obtained through simulations. However, the limited time and space were a constraint that meant many of these had to be excluded. After learning the math behind these concepts, I was very excited by the apparent potential of developing a new formula myself. Although it required multiple days of failures and correcting approaches, I was extremely happy when I finalized a formula that not only was correct in its derivation, but also adhered perfectly by the variables posited through experiment in literature.

This meant I had to make the decision to reallocate my time towards analysing data in light of this theory rather than developing a unique correction formula, which was a difficult decision but ultimately the right one. This is because it led to the justification of a concept that could, if worked on, potentially be useful to research and engineering in the field too.

Upon completing the data analysis, I was somewhat disappointed when there was a large quantitative discrepancy between the results the formula predicted and those I obtained. These were noticeable in some unexpectedly slow experimental observations, but I was hoping these were anomalous to specific values, which unfortunately was not the case.

First, I had to understand whether the error was in experiment or in theory. I did so by extrapolating literature data presented in direct graphic form, using a different variable. This seemed unreliable and I was uncertain about if it would be indicative of much. However, it did qualitatively appear to support the hypothesis that the theoretical formula was erroneous. I then had to consider why this was so, which revealed plausible concepts whose analysis I could not have incorporated into this experimental design. If I were to restart or study further, I would try to model these effects theoretically and incorporate these into my theory, as well as execute the statistical and more rigorous experimental procedures I had in mind earlier.

Following the finishing of my draft, my supervisor helped me review at the essay from the perspective of someone who has not spent time exploring these concepts, and bring clarity to both the KQ and introductory elements of the essay. Doing so contributed to my communication skills where the aspect of presenting research and new information is concerned. Overall, the entire process was very gratifying, both in furthering my research skills and experience, as well as approach to choosing and making the most of appropriate research topics from a practical standpoint too. I am happy with the work I have done and am hopeful to perhaps address many of the further questions and facets that I was unable to include in the essay independently.

How does the relative radius of a sphere affect the relative drag force it experiences in a bounded medium?

10.2. Derivation of Equation (21)

$$u = \left(\frac{1}{2\eta}\right)\left(\frac{dp}{dx}\right)y^2 + c_1 y + c_2 \qquad (10.2.1 = 20)$$

Given the no-slip condition, $u = 0$ at $y = 0$ and $y = h$.

$$0 = \left(\frac{1}{2\eta}\right)\left(\frac{dp}{dx}\right)(0) + c_1(0) + c_2 \qquad (10.2.2)$$

$$c_2 = 0 \qquad (10.2.3)$$

$$0 = \left(\frac{1}{2\eta}\right)\left(\frac{dp}{dx}\right)(h^2) + c_1(h) \qquad (10.2.4)$$

$$-\left(\frac{1}{2\eta}\right)\left(\frac{dp}{dx}\right)(h^2) = c_1(h) \qquad (10.2.5)$$

$$c_1 = -\left(\frac{1}{2\eta}\right)\left(\frac{dp}{dx}\right)(h) \qquad (10.2.6)$$

Substituting c_1 into Equation (20):

$$u = \left(\frac{1}{2\eta}\right)\left(\frac{dp}{dx}\right)y^2 - \left(\frac{1}{2\eta}\right)\left(\frac{dp}{dx}\right)hy \qquad (10.2.7)$$

$$u = \left(\frac{1}{2\eta}\right)\left(\frac{dp}{dx}\right)\big(y(y-h)\big) \qquad (10.2.8 = 21)$$

10.3. Integration of Equation (31)

$$F_{friction(wall)} = \int_0^A \tau \sin\theta \, dA = \frac{-4\eta v}{r_0} \int_0^{2\pi} \int_0^{r_0} \frac{r^2}{R-r} \, dr \, d\phi \qquad (10.3.1 = 31)$$

First, the interior integral is solved using u-substitution:

$$\int_0^{r_0} \frac{r^2}{R-r} dr \qquad (10.3.2)$$

$$u = R - r \qquad (10.3.3)$$

$$\frac{du}{dr} = -1 \qquad (10.3.4)$$

$$dr = -du \qquad (10.3.5)$$

$$= -\int_0^{r_0} \frac{(R-u)^2}{u} du = -\int_0^{r_0} (\frac{R^2}{u} - 2R + u) du \qquad (10.3.6)$$

$$= -\left[R^2 \ln|u| - 2Ru + \frac{u^2}{2}\right]_0^{r_0} = -\left[R^2 \ln|R-r| - 2R(R-r) + \frac{(R-r)^2}{2}\right]_0^{r_0} \qquad (10.3.7)$$

$$= -\left[R^2 \ln|R-r_0| - 2R(R-r_0) + \frac{(R-r_0)^2}{2} - R^2 \ln|R| + 2R^2 - \frac{R^2}{2}\right] \qquad (10.3.8)$$

$$= -\left[R^2 \ln\left|\frac{R-r_0}{R}\right| + 2Rr_0 + \frac{R^2 - 2Rr_0 + r_0^2}{2} - \frac{R^2}{2}\right] \qquad (10.3.9)$$

$$= -\left[R^2 \ln\left|\frac{R-r_0}{R}\right| + 2Rr_0 + \frac{-2Rr_0 + r_0^2}{2}\right] \qquad (10.3.10)$$

$$= \left[R^2 \ln\left|\frac{R}{R-r_0}\right| - 2Rr_0 + \frac{2Rr_0 - r_0^2}{2}\right] \qquad (10.3.11)$$

Since no ϕ terms are contained in equation (A2.11), the exterior integral is only multiplication with 2π. $F_{friction(wall)}$ is found by multiplying this with $\frac{-4\eta v}{r_0}$, leading to:

$$\frac{-8\eta v}{r_0}\left[R^2 \ln\left|\frac{R}{R-r_0}\right| - 2Rr_0 + \frac{2Rr_0 - r_0^2}{2}\right] \qquad (10.3.12)$$

As drag is a resistive force, the value is negative. The magnitude hence is:

$$\frac{8\eta v}{r_0}\left[R^2 \ln\left|\frac{R}{R-r_0}\right| - 2Rr_0 + \frac{2Rr_0 - r_0^2}{2}\right] \qquad (10.3.13 = 32)$$

How does the relative radius of a sphere affect the relative drag force it experiences in a bounded medium?

10.4. Vernier Calliper Measurements

Ball Radius $(r_0)/cm$		
Main Scale/cm	**Vernier Scale/cm**	$(r_0 \pm 0.01)$cm
0.1	0.05	0.15
0.3	0.02	0.32
0.4	0.08	0.48
0.6	0.04	0.64
0.7	0.09	0.79
0.9	0.05	0.95
Tube Radius $(R)/cm$		
Main Scale	**Vernier Scale**	$(R \pm 0.01)$cm
1.2	0.05	1.25

Table 10.4.1 – Vernier Calliper Measurements

10.5. Temperature Dependence of Density – Interpolation

Data for the variation of glycerol density with temperature and percentage (by weight) of glycerol was extracted from literature[33]. The data used for 100%Wt Glycerol is tabulated below. No uncertainties from the literature values were provided.

Temperature(T)/℃	Density/gcm^{-3}	Density $(\rho)/kgm^{-3}$
0	1.18273	1182.73
10	1.15604	1156.04
20	1.13018	1130.18
30	1.10388	1103.88
40	1.07733	1077.33
50	1.05211	1052.11
60	1.02735	1027.35
70	1.00392	1003.92
80	0.98181	981.81
90	0.95838	958.38

Table 10.5.1 – Density vs Temperature (Literature)

[33] Glycerine Producers' Association. Physical properties of glycerine and its solutions. Glycerine Producers' Association, 1963.

In order to determine the density (with uncertainties) at $T = 25°C$, this was linearly modelled, yielding a high R^2 value of 0.999.

$$\rho = 2.50T + 954.88 \tag{10.5.1}$$

At $T = 25°C$, this equates to $\rho = 1017.38\ kgm^{-3}$. Uncertainties were calculated on the basis of the experimental uncertainty in T, which was $\pm 0.25°C$ in an analogue thermometer. The uncertainty in density is equal to the difference between ρ when $T = 25.25°C$ and ρ when $T = 25°C$. In a linear model, this is identical to the difference between ρ when $T = 25°C$ and ρ when $T = 24.75°C$ too. Hence:

$$\Delta\rho = 2.50(25.25) - 2.50(25) = 0.625kgm^{-3} \approx 0.63kgm^{-3} \tag{10.5.2}$$

Hence: $\rho = (1017.38 \pm 0.63)kgm^{-3}$.

10.6. Temperature Dependence of Viscosity – Interpolation

The same analysis was carried out for glycerol (100%wt) viscosity and temperature, with data extracted from literature[34]. This is tabulated below. The units were converted from centipoises (*cP*) to Pascal-seconds (Pas) by dividing by 1×10^6. No uncertainties from the literature values were provided.

Temperature(T)/°C	**Viscosity/cP**	**Viscosity (η)/PaS**
0	12070000	12.07
10	3900000	3.90
20	1410000	1.41
30	612000	0.612
40	284000	0.284

Table 10.6.1 – Viscosity vs Temperature (Literature)

These were modelled using a polynomial of order 4. This is graphed below.

[34] Glycerine Producers' Association. Physical properties of glycerine and its solutions. Glycerine Producers' Association, 1963.

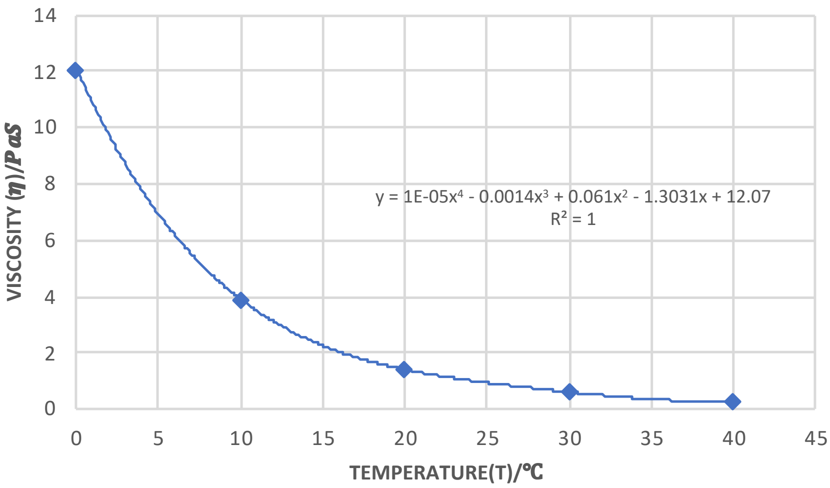

Graph 10.6.1 – Viscosity vs Temperature Data (Literature)

$$\eta = 0.00001153T^4 - 0.001356T^3 + 0.06102T^2 - 1.303T + 12.07 \qquad (10.6.1)$$

At $T = 25$°C, this equates to $\eta = 0.9489Pas$. The uncertainty is computed by finding the difference between $\eta(T = 25.25)$ and $\eta(T = 24.75)$, and dividing this by 2.

$$\Delta\eta = \frac{\eta(T = 25.25) - \eta(T = 24.75)}{2} = \frac{0.9674 - 0.9306}{2} = 0.0184\ Pas$$

Hence, at $T = 25$°C:

$$\eta = (0.9489 \pm 0.0184)\ Pa\ s$$

10.7. Uncertainty in *c*

$$c = \frac{r_0}{R} \qquad (10.7.1)$$

$$\frac{\Delta c}{c} = \frac{\Delta r_0}{r_0} + \frac{\Delta R}{R} \qquad (10.7.2)$$

$\frac{\Delta R}{R}$ is a constant as only one value of R is used:

$$\frac{\Delta R}{R} = \frac{0.01cm}{1.25cm} = 0.008$$

$\frac{\Delta r_0}{r_0}$ is dependent on each value of r_0, with Δr_0 constant at 0.01cm. These values are tabulated below, and each corresponding value of $\frac{\Delta c}{c}$ is computed.

Ball Radius (r_0/cm)	**Fractional Uncertainty in** r_0 $\left(\frac{\Delta r_0}{r_0}\right)$	**Fractional Uncertainty in Relative Radius** ***c*** $\left(\frac{\Delta c}{c}\right)$	**Absolute Uncertainty in Relative Radius** ***c*** Δc
0.15	0.067	0.075	0.0090
0.32	0.031	0.039	0.010
0.48	0.021	0.029	0.011
0.64	0.016	0.024	0.012
0.79	0.013	0.021	0.013
0.95	0.011	0.019	0.014

Table 10.7.1 – Uncertainty Computation for c

10.8. Uncertainties in Theoretical Values

$$k_{drag} = \frac{4}{3c^2}\ln\left|\frac{1}{1-c}\right| - \frac{4}{3c} + \frac{1}{3} \qquad (10.8.1 = 38)$$

To find Δk_{drag}, k_{drag} terms containing *c* can be separated:

$$A = \frac{4}{3c^2}\ln\left|\frac{1}{1-c}\right| \qquad (10.8.2)$$

$$B = \frac{4}{3c} \qquad (10.8.3)$$

$$k_{drag} = A - B + \frac{1}{3} \qquad (10.8.4)$$

$$\Delta k_{drag} = \Delta A + \Delta B \qquad (10.8.5)$$

Term A can be separated into two terms multiplied together:

$$T_1 = \frac{4}{3c^2} \qquad (10.8.6)$$

$$T_2 = \ln\left|\frac{1}{1-c}\right| \qquad (10.8.7)$$

$$\frac{\Delta A}{A} = \frac{\Delta T_1}{T_1} + \frac{\Delta T_2}{T_2} \qquad (10.8.8)$$

The fractional uncertainty in T_1 $(\frac{\Delta T_1}{T_1})$ is equal to the fractional uncertainty of the reciprocal:

$$\frac{\Delta T_1}{T_1} = \frac{\Delta(0.75c^2)}{(0.75c^2)} = 2\frac{\Delta c}{c} \qquad (10.8.9)$$

The absolute uncertainty of T_2 (ΔT_2) is equal to the fractional uncertainty of what is inside the logarithm ($\frac{1}{1-c}$).

$$\Delta T_2 = \frac{\Delta\left(\frac{1}{1-c}\right)}{\left(\frac{1}{1-c}\right)} \qquad (10.8.10)$$

By the reciprocal rule of fractional uncertainties:

$$\Delta T_2 = \frac{\Delta(1-c)}{(1-c)} = \frac{\Delta c}{c} \qquad (10.8.11)$$

Therefore:

$$\frac{\Delta T_2}{T_2} = \frac{\frac{\Delta c}{c}}{\ln\left|\frac{1}{1-c}\right|} \qquad (10.8.12)$$

$$\frac{\Delta A}{A} = 2\frac{\Delta c}{c} + \frac{\frac{\Delta c}{c}}{\ln\left|\frac{1}{1-c}\right|} \qquad (10.8.13)$$

$$\Delta A = \left(2\frac{\Delta c}{c} + \frac{\frac{\Delta c}{c}}{\ln\left|\frac{1}{1-c}\right|}\right) \times \frac{4}{3c^2}\ln\left|\frac{1}{1-c}\right| \qquad (10.8.14)$$

Term B has fractional uncertainty equivalent to the reciprocal:

$$\frac{\Delta B}{B} = \frac{\Delta(0.75c)}{(0.75c)} = \frac{\Delta c}{c} \qquad (10.8.15)$$

$$\Delta B = \frac{\Delta c}{c} \times \frac{4}{3c} \qquad (10.8.16)$$

Hence:

How does the relative radius of a sphere affect the relative drag force it experiences in a bounded medium?

$$\Delta k_{drag} = \left(2\frac{\Delta c}{c} + \frac{\frac{\Delta c}{c}}{\ln\left|\frac{1}{1-c}\right|} \right) \times \frac{4}{3c^2}\ln\left|\frac{1}{1-c}\right| + \left(\frac{\Delta c}{c} \times \frac{4}{3c}\right) \qquad (10.8.17)$$

This was computed for each value of *c*.

Relative Radius (c)	Absolute Uncertainty in Relative Drag Δk_{drag}
0.12	9.55
0.254	1.48
0.381	0.62
0.508	0.36
0.635	0.25
0.762	0.20

Table 10.8.1 - $\Delta \boldsymbol{k_{drag}}$ values.

The uncertainties are non-intuitive due to the formula's complexity.